



## Extensive glaciation in Transbaikalia, Siberia, at the Last Glacial Maximum



Martin Margold <sup>a,\*</sup>, John D. Jansen <sup>a,1</sup>, Artem L. Gurinov <sup>b</sup>, Alexandru T. Codilean <sup>c</sup>, David Fink <sup>d</sup>, Frank Preusser <sup>a,2</sup>, Natalya V. Reznichenko <sup>e</sup>, Charles Mifsud <sup>d</sup>

<sup>a</sup> Department of Physical Geography, Stockholm University, SE-106 91, Stockholm, Sweden

<sup>b</sup> Department of Geomorphology & Palaeogeography, Lomonosov Moscow State University, Leninskie gory, GSP-1, Moscow, 119991, Russian Federation

<sup>c</sup> School of Earth & Environmental Sciences, University of Wollongong, Northfields Avenue, Wollongong, NSW, 2522, Australia

<sup>d</sup> Institute for Environmental Research, Australian Nuclear Science & Technology Organisation, Locked Bag 2001, Kirrawee DC, NSW, 2232, Australia

<sup>e</sup> Department of Geography, Durham University, Lower Mountjoy, South Road, Durham, DH1 3LE, UK

### ARTICLE INFO

#### Article history:

Received 27 March 2015

Received in revised form

23 November 2015

Accepted 26 November 2015

Available online 14 December 2015

#### Keywords:

Glaciation

Transbaikalia

Last Glacial Maximum

Cosmogenic <sup>10</sup>Be exposure dating

Optically stimulated luminescence

### ABSTRACT

Successively smaller glacial extents have been proposed for continental Eurasia during the stadials of the last glacial period leading up to the Last Glacial Maximum (LGM). At the same time the large mountainous region east of Lake Baikal, Transbaikalia, has remained unexplored in terms of glacial chronology despite clear geomorphological evidence of substantial past glaciations. We have applied cosmogenic <sup>10</sup>Be exposure dating and optically stimulated luminescence to establish the first quantitative glacial chronology for this region. Based on eighteen exposure ages from five moraine complexes, we propose that large mountain ice fields existed in the Kodar and Udokan mountains during Oxygen Isotope Stage 2, commensurate with the global LGM. These ice fields fed valley glaciers (>100 km in length) reaching down to the Chara Depression between the Kodar and Udokan mountains and to the valley of the Vitim River northwest of the Kodar Mountains. Two of the investigated moraines date to the Late Glacial, but indications of incomplete exposure among some of the sampled boulders obscure the specific details of the post-LGM glacial history. In addition to the LGM ice fields in the highest mountains of Transbaikalia, we report geomorphological evidence of a much more extensive, ice-cap type glaciation at a time that is yet to be firmly resolved.

© 2015 Elsevier Ltd. All rights reserved.

### 1. Introduction

The glacial history of northern Eurasia has displayed opposing trends between its western, central and eastern parts during the last glacial cycle. Whereas the Fennoscandian Ice Sheet reached close to its maximum Pleistocene extent at the Last Glacial Maximum (LGM; in Oxygen Isotope Stage [OIS] 2), the continental

sector of the Barents-Kara Ice Sheet and smaller Eurasian ice masses to the east show a sequence of successively diminishing glacial advances (stadials) during the course of the last glacial cycle (Svendsen et al., 2004; Stauch and Gualtieri, 2008; Astakhov, 2013). In order to better understand this apparent anti-phase behaviour between the Fennoscandian and Barents-Kara ice sheets, we focus on major glaciated massifs in a remote area of Eurasia for which information is wholly lacking.

Extensive mountain glaciation is documented for southern Siberia, north-western Mongolia, and north-western China (Lehmkuhl et al., 2011) where valley glacier advances are reported for OIS-6 and -2 via optically stimulated luminescence and cosmogenic nuclide exposure dating (Lehmkuhl et al., 2004, 2007; Gillespie et al., 2008; Arzhannikov et al., 2012; Zhao et al., 2013). Despite some regional differences in the relative prominence of glacial advances during different cold periods, the general trend in the Altai and Sayan mountains, located south of the maximum continental limit of the Barents-Kara Ice Sheet, is for progressively

\* Corresponding author.

E-mail addresses: [martin.margold@natgeo.su.se](mailto:martin.margold@natgeo.su.se) (M. Margold), [john.jansen@uni-potsdam.de](mailto:john.jansen@uni-potsdam.de) (J.D. Jansen), [gurinov.artem@gmail.com](mailto:gurinov.artem@gmail.com) (A.L. Gurinov), [codilean@uow.edu.au](mailto:codilean@uow.edu.au) (A.T. Codilean), [david.fink@ansto.gov.au](mailto:david.fink@ansto.gov.au) (D. Fink), [frank.preusser@geologie.uni-freiburg.de](mailto:frank.preusser@geologie.uni-freiburg.de) (F. Preusser), [natalya.reznichenko@durham.ac.uk](mailto:natalya.reznichenko@durham.ac.uk) (N.V. Reznichenko), [charles.mifsud@ansto.gov.au](mailto:charles.mifsud@ansto.gov.au) (C. Mifsud).

<sup>1</sup> Present address: Institute of Earth & Environmental Science, University of Potsdam, Karl-Liebknecht-Str. 24-25, 14476 Potsdam-Golm, Germany.

<sup>2</sup> Present address: Institute of Earth and Environmental Sciences, Albert-Ludwigs-Universität Freiburg, Albertstr. 23-B, 79104 Freiburg, Germany.

smaller glaciations since OIS-6 (Fig. 1; Gillespie et al., 2008; Lehmkuhl et al., 2011; Arzhannikov et al., 2012; Zhao et al., 2013). A large ice cap that existed in the central Sayan-Tuva Upland in OIS-6 and -4 was apparently absent during OIS-3 and -2 when the character of glaciation changed to branching valley glaciers (Komatsu et al., 2007b; Arzhannikov et al., 2012). In the Khangai Mountains of west-central Mongolia, the most extensive preserved moraine ridges date to OIS-3 with OIS-2 ice limits reaching nearly the same extents (Rother et al., 2014). An even stronger trend of successively diminishing glacial advances is documented for the Verkhoyansk Mountains, a large mountain group east of the Aldan and Lena rivers in eastern Siberia (Fig. 1). Here moraine complexes dated with infrared optically stimulated luminescence indicate minimal ice masses during the (global) LGM (Stauch et al., 2007; Stauch and Gualtieri, 2008; Stauch and Lehmkuhl, 2010).

Transbaikalia, situated between the Sayan and Verkhoyansk mountains, is a vast mountainous region east of Lake Baikal where intermontane basins of the Baikal Rift Zone are surrounded by massifs with alpine relief (Figs. 1 and 2; Shahgedanova et al., 2002). The region displays significant glacial modification but little information is available concerning ice extent or chronology (Shahgedanova et al., 2002; Margold and Jansson, 2011). Here we investigate the timing of glaciations in central Transbaikalia with particular focus on the Kodar Mountains, the region's highest massif. Based on cosmogenic  $^{10}\text{Be}$  exposure dating and optically stimulated luminescence (hereafter abbreviated to exposure dating and OSL, respectively), we propose a framework for the extent and timing of the last glaciation and thus provide a new perspective on

the nature of the LGM in northern Eurasia.

## 2. Transbaikalia, Siberia

The mountains of Transbaikalia, including those surrounding Lake Baikal, form a region of high-relief stretching more than 1000 km along a west-east axis between 108 and 121° E (Fig. 1). The mountain crux of the region is located between 58 and 55° N where peaks ~3000 m above sea level (asl) stand more than 2000 m above the surrounding extensional depressions of the Baikal Rift (Figs. 2 and 3). Lower mountains (<2000 m asl) are bounded to the north by the River Lena at about 58° N, and south of 55–56° N sees the rolling terrain of the Vitim Plateau. The regional climate is boreal, with continentality and precipitation following a northwest-southeast (drying) gradient consistent with being at the eastern-most fringe of west-derived moisture (Geniatulin, 2000).

### 2.1. Glacial history

Evidence of past glaciation was first recognised in Transbaikalia by Kropotkin (1876) who described traces of past glaciations in the mountains of northern Transbaikalia down to 630 m asl. Describing the mountains of the region, Obruchev (1923, 1932) distinguished two glacial events and suggested that “glaciers had an alpine character in more mountainous areas, while in plateau and highland areas they were close to Scandinavian type” (Obruchev, 1923, p. 34). Despite more intensive field research after 1945 motivated by mineral exploration and infrastructure projects, no consistent

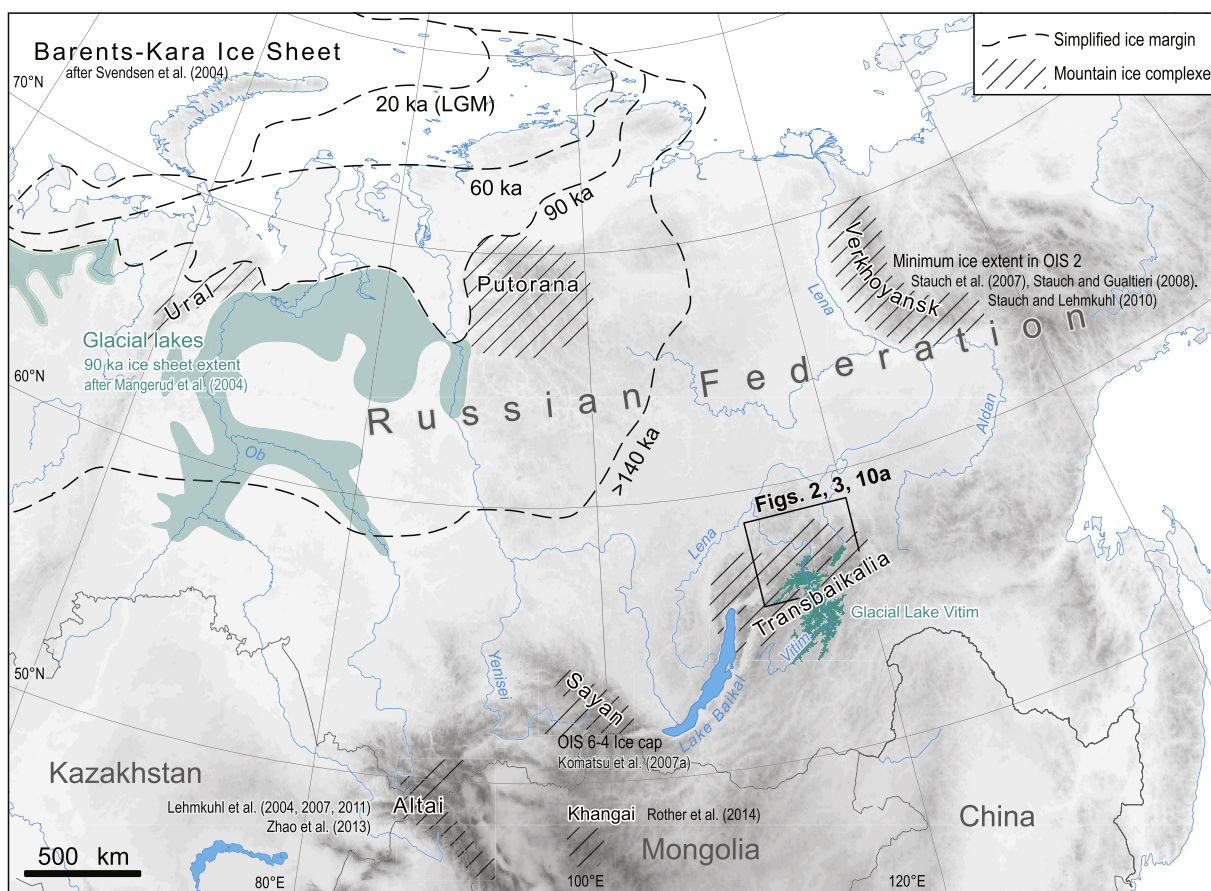


Fig. 1. Study area location within northern Eurasia plus information on the glacial history of the wider region. Location of Figs. 2 and 3 is indicated by a black rectangle (Mangerud et al., 2004).

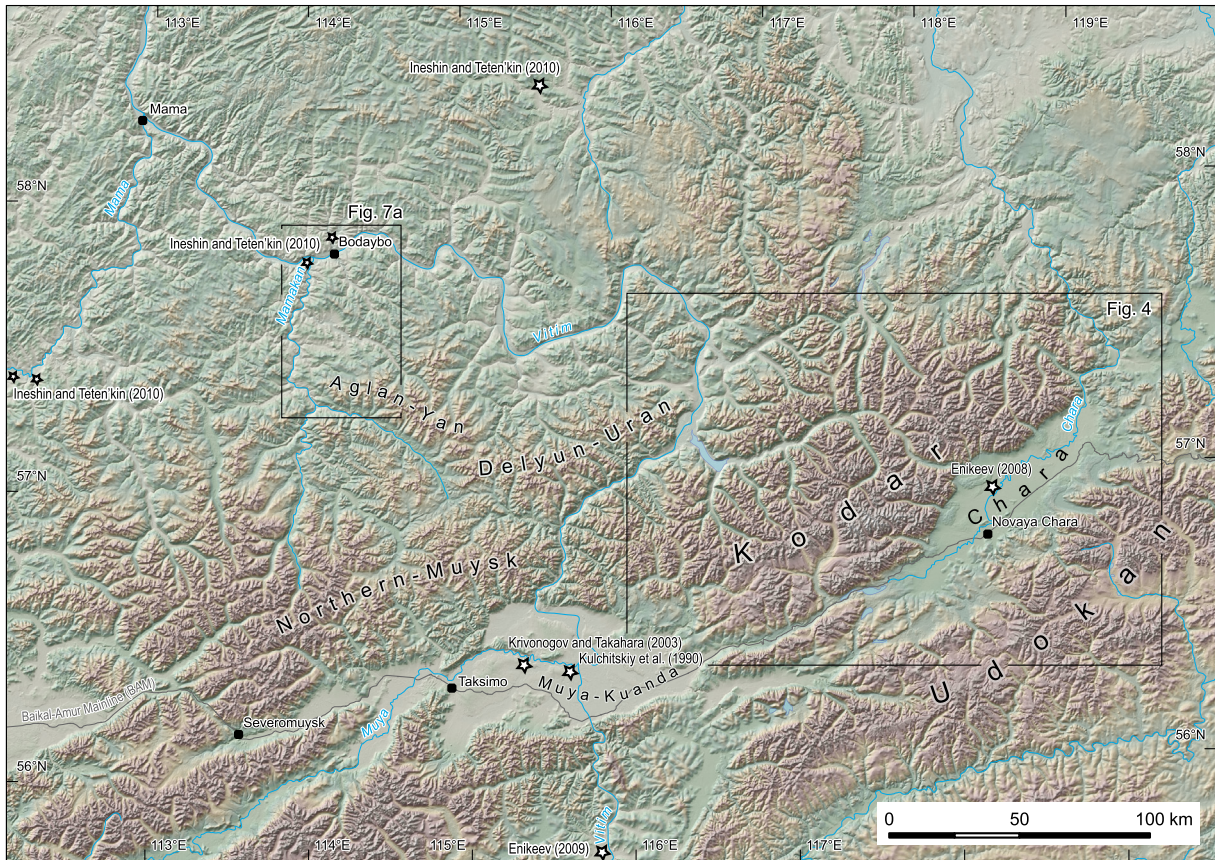


Fig. 2. Study area. Locations of Figs. 4 and 7 are indicated by black rectangles; sites of radiocarbon dates discussed in the text are marked by stars.

picture was to emerge regarding the glacial history of the region. Opinions varied widely both in terms of the intensity of glaciation and its timing. Logatchev (1974) suggested two glacial stages: Samarovo (Middle Pleistocene) of valley glacier or ice-cap type, and Zyryanka (Late Pleistocene), which included several stages of valley glaciation. In contrast, Zolotarev (1974) suggested two stages of valley glaciers during the middle Pleistocene, with the possibility that some glacial sediments were of Early Pleistocene age, followed by a more intensive glaciation in the early-Late Pleistocene when an ice cap might have been present in the Bodaybo region (Figs. 2 and 3). The timing of this latter stage was determined by fossil fragments. Climate during the LGM (Sartan stadial according to the regional chronology) was too arid for the development of larger ice masses, according to Zolotarev (1974), but valley glaciers existed in the highest ranges.

More recent investigations of the sedimentary record within the intermontane basins seem to confirm two glacial stages in the Middle Pleistocene plus two stages during the Late Pleistocene (Bazarov et al., 1981; Bazarov, 1986; Enikeev, 2008, 2009). In addition, the intermontane basins Muya-Kuanda and Chara (Figs. 2 and 3) are described as having been repeatedly filled by lakes and, although their origin remains disputed (cf. Kulchitskiy et al., 1995; Ufimtsev et al., 1998; Kolomiets, 2008), many agree that the damming of rivers by glaciers was responsible (Osadchiy, 1979, 1982; Krivonogov and Takahara, 2003; Enikeev, 2008, 2009; Margold and Jansson, 2011; Margold et al., 2011)—as suggested by the pioneering work of Obruchev (1929).

None of the studies above provide chronological constraints on the regional Quaternary glacial stratigraphy. Quantitative dating available for the study area consists solely of  $^{14}\text{C}$  and is summarised

below (all  $^{14}\text{C}$  ages are calibrated using IntCal13 [Reimer et al., 2013] calibration curve in Calib 7.0 online calibration calculator [Stuiver and Reimer, 1993]; uncertainties are reported at  $1\sigma$ , with ages rounded to the nearest 10 cal yrs; original uncalibrated  $^{14}\text{C}$  ages and laboratory numbers are given in parentheses)<sup>3</sup>.

- 1) Three samples are available for the Muya-Kuanda depression: 44,820–43,270 cal yrs BP (40,500  $\pm$  930  $^{14}\text{C}$  yrs BP; SOAN-2893), and 42,880–41,860 cal yrs BP (38,320  $\pm$  755  $^{14}\text{C}$  yrs BP; SOAN-2823) from a palaeosol in the bank of the Muya River (Krivonogov and Takahara, 2003), and 43,360–37,350 cal yrs BP (36,480  $\pm$  3130  $^{14}\text{C}$  yrs BP; SOAN-2483) on a piece of wood from the vicinity of the Mudirikan and Muya river confluence (Kulchitskiy et al., 1990; see Fig. 2 for the locations).
- 2) One sample, dated to 29,950–27,960 cal yrs BP (24,730  $\pm$  770  $^{14}\text{C}$  yrs BP; SOAN-2979) from a piece of wood underlying lacustrine sediments at the mouth of the Bambuyka river in the Vitim River catchment upstream of the Muya-Kuanda Depression (Enikeev, 2009; see our Fig. 2).
- 3) A 1180 m deep drill-core in the Chara Depression, thought to span the Pliocene and Pleistocene, is constrained by one date of 42,960–41,750 cal yrs BP (38,210  $\pm$  870  $^{14}\text{C}$  yrs BP; LU-977) on a piece of wood, identifying OIS-3 sediments at 41.1–73 m depth (Enikeev, 2008).
- 4) A large number of radiocarbon dates are available from several sites in the northwest portion of the study area, largely from

<sup>3</sup> We note that several of the reported  $^{14}\text{C}$  ages approximate the ~40–35 kyr limit of conventional  $^{14}\text{C}$  dating and therefore possibly reflect a minimum age.

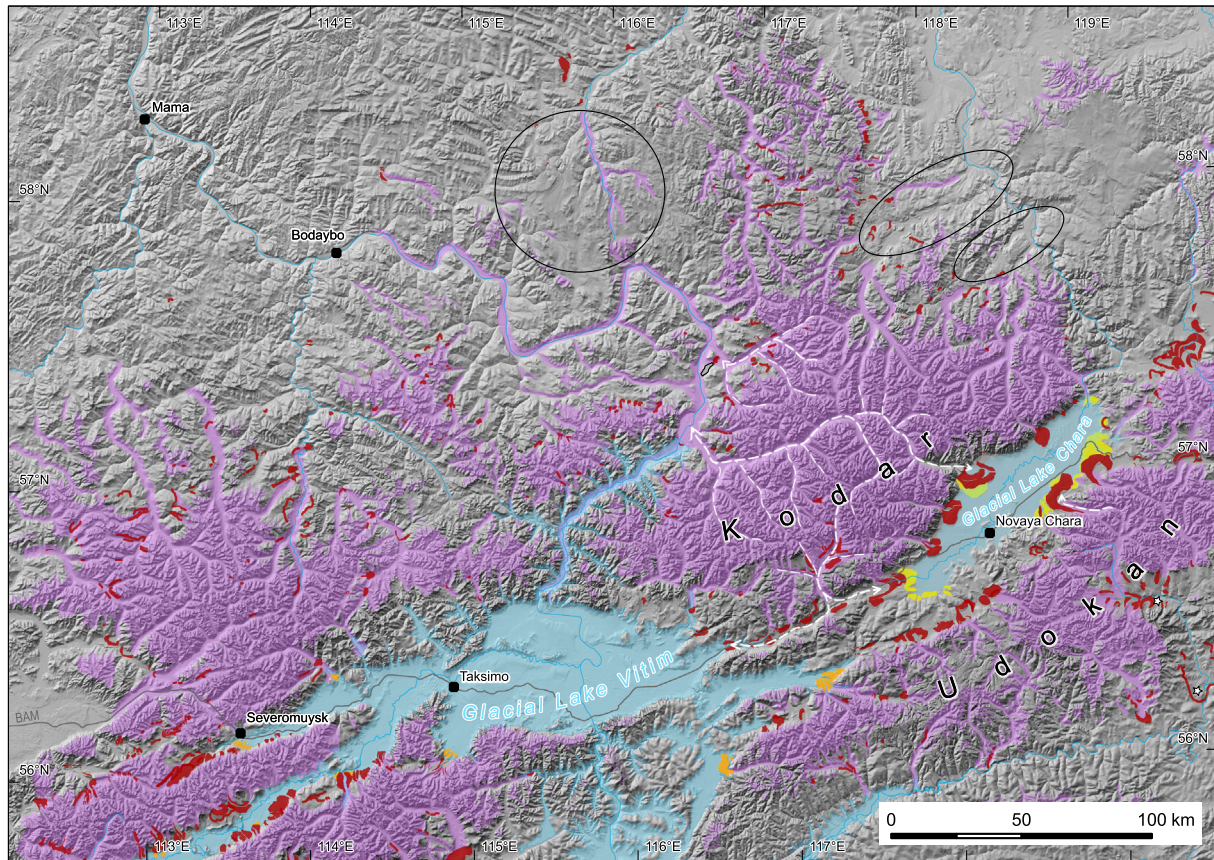


**Fig. 3.** Mapped glacial geomorphology redrawn from Margold and Jansson (2011). Glacially modified terrain (U-shaped valleys, cirques, arêtes) is shaded purple, moraines in dark red, deltas in orange, indistinct deltas in yellow, and glacial lakes in blue. White dashed lines indicate the branching valley glaciers on whose moraines we collected samples for  $^{10}\text{Be}$  exposure dating. A circle in the highlands northeast of Bodaybo as well as two ellipses on the northeast slopes of the Kodar Mountains indicate zones of areal glacial scouring (after Margold and Jansson, 2011). Note two distinct generations of moraines in the main valley draining the Udokan Mountains to the south-southeast (marked by white stars). (For interpretation of the references to colour in this figure legend, the reader is referred to the web version of this article.)

archaeological research locales (Ineshin and Teten'kin, 2010). Those relevant for the regional glacial history are: (i) a pair of dates from the valley of the Karenga River (a tributary of the Mama River; Fig. 2) on bones embedded in “moraine-like” sediments dated to 20,990–20,700 cal yrs BP ( $17,290 \pm 100$   $^{14}\text{C}$  yrs BP; GIN-8983) and 29,370–27,900 cal yrs BP ( $24,600 \pm 730$   $^{14}\text{C}$  yrs BP; SOAN-4422), with several other dates falling into a broader LGM period derived from bones and mammoth tusks embedded in laminated lacustrine sediments in the adjacent tributary valleys of the Mama River; (ii) a date on charcoal from an exposed section at the Vitim River, 1 km south of the Mamakan River mouth, dated to 23,270–21,850 cal yrs BP ( $18,670 \pm 600$   $^{14}\text{C}$  yrs BP; SOAN-4546) and a date on bone from an exposed section at the Bodaybo River 2 km upstream from its mouth, giving 27,090–26,090 cal yrs BP ( $22,300 \pm 500$   $^{14}\text{C}$  yrs BP; GIN-8878; Fig. 2); (iii) a group of ages on bones and wood from alluvial sediments on the Vacha River, in the area northeast of Bodaybo (Fig. 2) spanning ~35,240 cal yrs BP (~33,000  $^{14}\text{C}$  yrs BP) to beyond the  $^{14}\text{C}$  limit (Ineshin and Teten'kin, 2010).

The lack of either geochronology or systematic mapping of the glacial geomorphology has kept Transbaikalia as an empty space on the map between the more closely studied regions of the south Siberian mountains (e.g., Lehmkuhl et al., 2004; Komatsu et al., 2007a, b; Lehmkuhl et al., 2007; Gillespie et al., 2008; Lehmkuhl et al., 2011; Arzhannikov et al., 2012; Zhao et al., 2013) and the mountains of far north-east Russia and the Kamchatka peninsula

(e.g., Brigham-Grette, 2001; Bigg et al., 2008; Stauch et al., 2007; Stauch and Gualtieri, 2008; Stauch and Lehmkuhl, 2010; Barr and Clark, 2011, 2012). This knowledge gap motivated the mapping survey of Margold and Jansson (2011) together with field-based efforts, reported here, to establish quantitative age control on glacialiations in central Transbaikalia with  $^{10}\text{Be}$ -derived exposure dating.

## 2.2. Field sites

Our study centres on the Kodar Mountains, the highest massif in the region, which currently hosts over 30 small cirque glaciers (Preobrazhenskiy, 1960; Shahgedanova et al., 2002, 2011; Stokes et al., 2013; Osipov and Osipova, 2014). We collected samples for exposure dating from boulders on moraine complexes in the Chara Depression and in the River Vitim valley (Table 1; Fig. 4). In the Chara Depression samples derive from: (i) inner (V-12-MM-01 to 03) and outer (V-12-MM-04 to 06) ridges of the Apsat River moraine complex (Figs. 4 and 5a); (ii) inner (V-12-MM-12 to 14) and outer (V-12-MM-10 and 11) ridges of the Leprindo Lakes moraine complex (Figs. 4 and 5b); and (iii) the Ikabja moraine, located on the southern boundary of the Chara Depression and formed by a glacier flowing from the Udokan Range (V-12-MM-07 to 09; Figs. 4 and 5c). In the Vitim River valley, northwest of the Kodar Mountains, we sampled a moraine formed by a glacier emanating from the Lake Oron valley (GLV-11 and 13; Figs. 4 and 6a), and the Baznyi moraine formed by a glacier in the Amalyk River valley (V-12-MM-16 to 17; Figs. 4 and 6b) just northeast of a

**Table 1**  
Cosmogenic  $^{10}\text{Be}$  sample data and modelled surface exposure ages.

Location Sample code	Latitude/Longitude (°N/°E)	Elevation (m above sea level)	Sample thickness <sup>a</sup> (cm)	Topographic shielding factor	Height of boulder above ground (cm)	Quartz <sup>b</sup> Mass (g)	Be carrier mass (mg)	$^{10}\text{Be}/^9\text{Be}^c$ ( $\times 10^{-15}$ )	$^{10}\text{Be}$ Concentration <sup>c</sup> ( $\times 10^3$ atoms $\text{g}^{-1}$ $\text{SiO}_2$ )	Age <sup>c, d</sup> (ka)
Apsat moraine inner crest										
V-12-MM-01	56.98518/118.15501	936	3	1	80	33.20	0.345	88.4 ± 4.3	61.40 ± 3.29	6.3 ± 0.5
V-12-MM-02	56.98513/118.15450	926	3	1	100	30.60	0.344	203.5 ± 7.0	152.90 ± 6.27	16.0 ± 1.1
V-12-MM-03	56.98460/118.15321	927	3	1	120	29.47	0.340	281.8 ± 6.3	217.26 ± 6.87	22.8 ± 1.4
Apsat moraine outer crest										
V-12-MM-04	56.99836/118.30656	805	2	1	60	35.11	0.338	177.8 ± 5.3	114.39 ± 4.27	13.2 ± 0.8
V-12-MM-05	57.00034/118.31067	782	2.5	1	110	32.13	0.341	94.5 ± 3.9	67.03 ± 3.12	7.9 ± 0.5
V-12-MM-06	57.00052/118.31419	767	1	1	60	29.41	0.341	79.7 ± 5.0	61.75 ± 4.11	7.3 ± 0.6
Leprindo moraine inner crest										
V-12-MM-12	56.60032/117.4916	1108	2	1	140	24.84	0.346	166.2 ± 9.7	154.72 ± 9.70	13.8 ± 1.1
V-12-MM-13	56.59451/117.49396	1142	3	1	40	12.43	0.346	77.6 ± 5.0	144.33 ± 9.83	12.6 ± 1.1
V-12-MM-14	56.60017/117.49263	1108	3	1	100	32.40	0.343	156.9 ± 9.0	111.00 ± 6.85	10.0 ± 0.8
Leprindo moraine outer crest										
V-12-MM-10	56.66717/117.67627	954	2	1	30	34.31	0.339	300.8 ± 8.3	198.66 ± 7.05	20.2 ± 1.3
V-12-MM-11	56.66788/117.67362	940	3	0.999	30	22.97	0.343	35.1 ± 3.4	35.03 ± 3.50	3.6 ± 0.4
Ikabja moraine										
V-12-MM-07	56.93895/118.69913	970	2.5	1	50	32.52	0.340	278.5 ± 10.8	194.58 ± 8.70	19.5 ± 1.3
V-12-MM-08	56.93906/118.69975	970	3	1	50	40.96	0.344	407.3 ± 11.8	228.60 ± 8.38	23.0 ± 1.5
V-12-MM-09	56.9398/118.70044	966	3.5	1	50	38.55	0.338	795.6 ± 14.3	466.26 ± 13.38	47.5 ± 2.8
Oron delta moraine										
GLV-11	57.15510/116.3327	436	2	0.998	80	37.62	0.736	248.0 ± 9.9	120.62 ± 4.93	19.7 ± 1.3
GLV-13	57.15567/116.33258	427	3	0.998	60	36.03	0.734	238.0 ± 9.3	120.79 ± 4.83	20.1 ± 1.3
Baznyi moraine										
V-12-MM-16	57.43035/116.57731	515	2	0.999	120	25.9	0.331	125.2 ± 3.0	107.03 ± 3.51	16.2 ± 1.0
V-12-MM-17	57.43903/116.5736	513	2	0.999	250	39.9	0.332	139.6 ± 3.9	77.53 ± 2.76	11.8 ± 0.7
Mamakan glacially eroded surface										
V-12-MM-15	57.82583/114.03742	394	3	0.999	–	28.2	0.332	152.3 ± 4.4	119.63 ± 4.38	20.5 ± 1.3

<sup>a</sup> The tops of all samples were exposed at the surface.

<sup>b</sup> A density of 2.7  $\text{g cm}^{-3}$  was used based on the granitic composition of the samples.

<sup>c</sup> All uncertainties are reported at the 1-sigma level. Blank corrected 10/9 ratios. See text for details on level of blanks.

<sup>d</sup> Exposure ages were calculated with the Cosmic-Ray Produced Nuclide Systematics (CRONUS) Earth online calculator (Balco et al., 2008) version 2.2; constants 2.2.1; (<http://hess.ess.washington.edu/>), using  $^{10}\text{Be}$  SLHL production rate of Heyman (2014). Full details of the cosmogenic  $^{10}\text{Be}$  analyses and exposure age calculations are provided in Section 3.1.

giant bedrock spillway associated with a glacial lake outburst flood (see Margold et al., 2011). All samples were of medium to coarse-grained granite lithology with the exception of GLV-13, which consisted of mica-schist.

With the aim of extending the knowledge of glaciations farther afield, we sampled a glacially eroded bedrock surface (coarse-grained granite) on a hillslope above the Vitim River opposite the town of Mamakan (V-12-MM-15; Fig. 7a–c) near Bodaybo. We also collected a sample for OSL analysis from glaciolacustrine sediments deposited behind a moraine in the Tamarak valley downstream of the Aglan-Yan, a minor range south of Bodaybo (TK-12-01; Figs. 2 and 7a, d–f). At this site, a ~20 m high section of upwards-coarsening diamicton is exposed in a road-side gravel pit (see Fig. 7f). At the eastern end of the section, several metres of stratified sediment grade up from clayey-silts at base to silts with intercalated sandy beds. We attribute this sequence to a minor proglacial lake, which formed when the drainage of a tributary valley coming from the NNE was blocked by a glacier lobe in the Tamarak River valley (see Fig. 7d).

### 3. Methods

#### 3.1. Cosmogenic $^{10}\text{Be}$ analyses

Samples for exposure dating were collected with a hammer and chisel, and sample coordinates and elevations were recorded via hand-held GPS (Table 1). Samples GLV-11 and GLV-13, collected in 2011, were processed at Deutsches GeoForschungsZentrum GFZ in Potsdam. Quartz was separated and cleaned following procedures based on Kohl and Nishiizumi (1992) and  $^{10}\text{Be}$  was extracted using

ion chromatography following procedures described by von Blanckenburg et al. (2004) and von Blanckenburg et al. (1996), using approximately 250  $\mu\text{g}$   $^9\text{Be}$  carrier solution prepared from phenakite mineral, with  $^9\text{Be}$  concentration of  $372.5 \pm 3.5$  ppm.  $^{10}\text{Be}/^9\text{Be}$  ratios of these two samples were measured at the University of Cologne's accelerator mass spectrometer laboratory (Dewald et al., 2013). The  $^{10}\text{Be}/^9\text{Be}$  ratio of the full procedural blank prepared with these samples was  $0.8 \pm 0.3 \times 10^{-15}$  and blank corrected  $^{10}\text{Be}/^9\text{Be}$  ratios obtained for GLV-11 and GLV-13 were  $2.5 \pm 0.1 \times 10^{-13}$  and  $2.4 \pm 0.1 \times 10^{-13}$ , respectively. The  $^{10}\text{Be}/^9\text{Be}$  ratios obtained for the two samples were normalised to the 2007 KNSTD standard (see Nishiizumi et al., 2007 and Balco et al., 2008 for more details).

The V-12-MM series of samples, collected in 2012, were processed at the Australian Nuclear Science and Technology Organisation (ANSTO) using a combination of standard HF/HNO<sub>3</sub> methods after Child et al. (2000) and hot phosphoric acid (Mifsud et al., 2013). All samples were spiked with a  $^{10}\text{Be}$ -free solution of approximately 300  $\mu\text{g}$   $^9\text{Be}$  prepared from a beryl crystal solution at 1080 ( $\pm 0.7\%$ ) ppm. Full procedural chemistry blanks were prepared from the same beryl and gave a final mean  $^{10}\text{Be}/^9\text{Be}$  ratio of  $13.2 \pm 1.5 \times 10^{-15}$  ( $n = 4$ , mean of two procedural blanks). Blank corrected  $^{10}\text{Be}/^9\text{Be}$  ratios ranged between 0.8 and  $8.0 \times 10^{-13}$  with analytical errors ranging from 2 to 6%. The  $^{10}\text{Be}/^9\text{Be}$  ratios were measured at the ANSTO ANTARES accelerator (Fink and Smith, 2007) and were normalised to the NIST SRM-4325 standard with a revised nominal  $^{10}\text{Be}/^9\text{Be}$  ratio of  $2.790 \times 10^{-11}$ . Errors for the final  $^{10}\text{Be}$  concentrations (atoms/g) were calculated by summing in quadrature the statistical error for the AMS measurement, 2% for reproducibility, and 1% for uncertainty in the Be spike

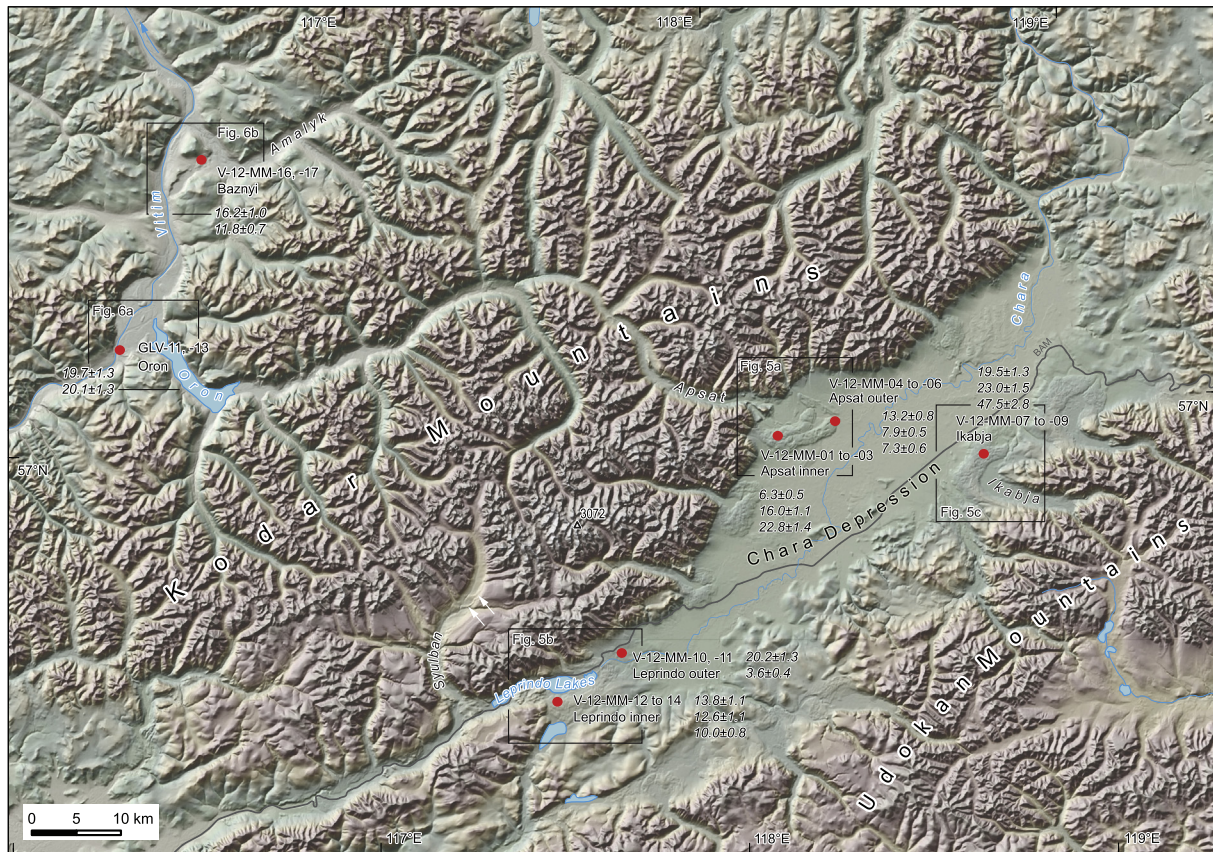


**Fig. 4.** Highest mountain ranges of central Transbaikalia, the Kodar and Udokan, surrounding the Chara Depression, and the Vitim River skirting the northwest slopes: DEM-derived image (Shuttle Radar Topography Mission, SRTM, data), showing dated moraines (red dots). Locations of Figs. 5 and 6 are marked by black rectangles. White arrows in the Syulban valley (Kodar Mountains; upstream from Leprindo Lakes) indicate identified recessional moraines. See Fig. 2 for the location within the overall study area. (For interpretation of the references to colour in this figure legend, the reader is referred to the web version of this article.)

concentration.

Exposure ages were calculated using the CRONUS online calculator (Balco et al., 2008; version 2.2; constants 2.2.1) and are reported here using the time-dependent CRONUS  $Lm^4$  production rate scaling of Lal (1991) and Stone (2000), with a reference spallation production rate of  $3.94 \pm 0.20$  atoms  $g^{-1} yr^{-1}$  (Heyman, 2014). The  $^{10}Be$  half-life of  $1.387 \pm 0.012$  Myr (Chmeleff et al., 2010; Korschinek et al., 2010) was used in all calculations.

### 3.2. Optically stimulated luminescence analyses

Sample TK-12-01 was collected using a stainless-steel tube hammered into the sediment profile and processed at the Stockholm University luminescence laboratory. Sediment from the outer part of the sample was used for gamma spectrometric measurements; cosmic ray dose was calculated using present-day depth and assuming average water content of  $40 \pm 5\%$  during burial, considering the fine-grained nature of the sediment and its position. Material from the inner part of the sample was sieved (63–100  $\mu m$ ) and chemically pre-treated (HCl,  $H_2O_2$ , Na-oxalate). The quartz fraction was isolated using heavy liquids, and then etched with 40% HF (60 min), followed by 10% HCl treatment (>120 min) and re-sieving. Equivalent dose ( $D_e$ ) was determined (Risø DA-20) using a modified version of the SAR-protocol of

Murray and Wintle (2000), with preheating at 230 °C for 10 s prior to all OSL measurements (blue diode stimulation for 60 s at 125 °C, Hoya U340 detection filter).

## 4. Results

The full set of  $^{10}Be$  analytical data and exposure ages are presented in Table 1 grouped according to location. Exposure ages from all sampled moraines display a relatively large spread (Table 1; Fig. 8), often up to a factor of two, despite total external errors of about  $\pm 7\%$ . For the Apsat River moraine complex (Figs. 4 and 5a), exposure ages from the inner moraine (V-12-MM-01, -02, -03) range from 23 to 6 ka, whereas for the outer moraine (V-12-MM-04, -05, -06) the range is 13 to 7 ka. A similar spread of 20 to 4 ka was obtained for the outer Leprindo moraine (V-12-MM-10, -11; Figs. 4 and 5b), whereas the ages for the inner Leprindo moraine (V-12-MM-12, -13, -14) were a more consistent 14 to 10 ka. Boulders sampled on the large Ikabja moraine (Figs. 4 and 5c) returned exposure ages of 48 to 20 ka (V-12-MM-07, -08, -09). The two boulders sampled on the small moraine directly in the Vitim River valley west of Lake Oron (GLV-11, -13; Figs. 4 and 6a) yielded overlapping ages (at  $1\sigma$ ) of 20 ka. Two boulders sampled on the Baznyi moraine in the Amalyk River valley (Figs. 4 and 6b) returned ages of 16 and 12 ka (V-12-MM-16, -17, respectively). The single bedrock sample collected from a glacially eroded surface across the Vitim River from Mamakan (Fig. 7a–c) yielded an exposure age of 21 ka.

For OSL sample TK-12-01, representing glaciolacustrine

<sup>4</sup> Adapting the Lal (1991) scaling scheme for paleomagnetic corrections. See Balco et al. (2008) for more details.

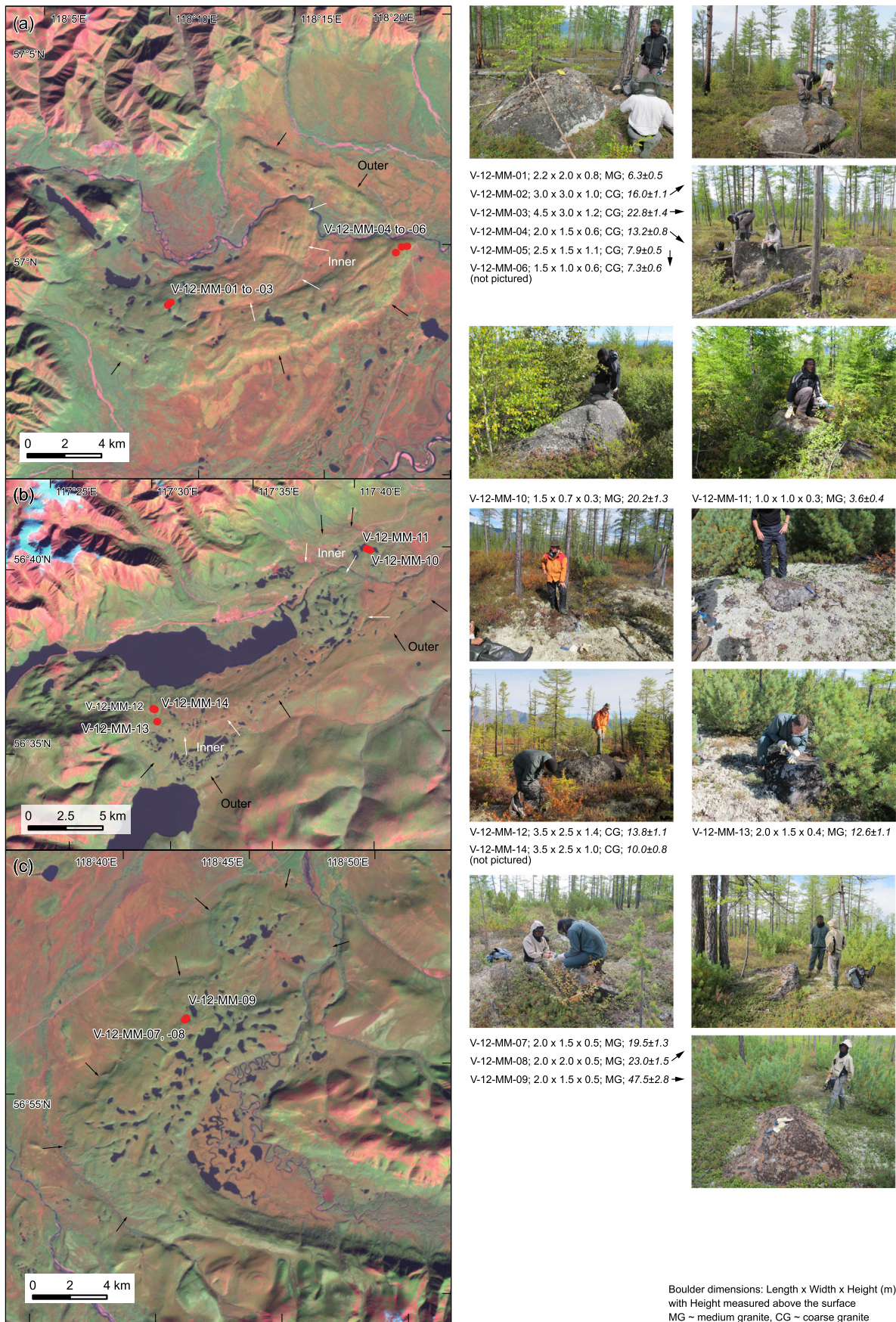


**Fig. 5.** Chara Depression moraine complexes with sampling sites (red dots): Landsat image (LE71290212000275SGS00; channels 5, 3, 1) draped over SRTM data. (a) Apsat moraines, (b) Leprindo Lakes moraines, (c) Ikabja moraine. Photographs to the right of the map panels show the sampled boulders. See Fig. 4 for the location of Fig. 5 map panels. Outlines of the moraine ridges are marked by arrows. (For interpretation of the references to colour in this figure legend, the reader is referred to the web version of this article.)

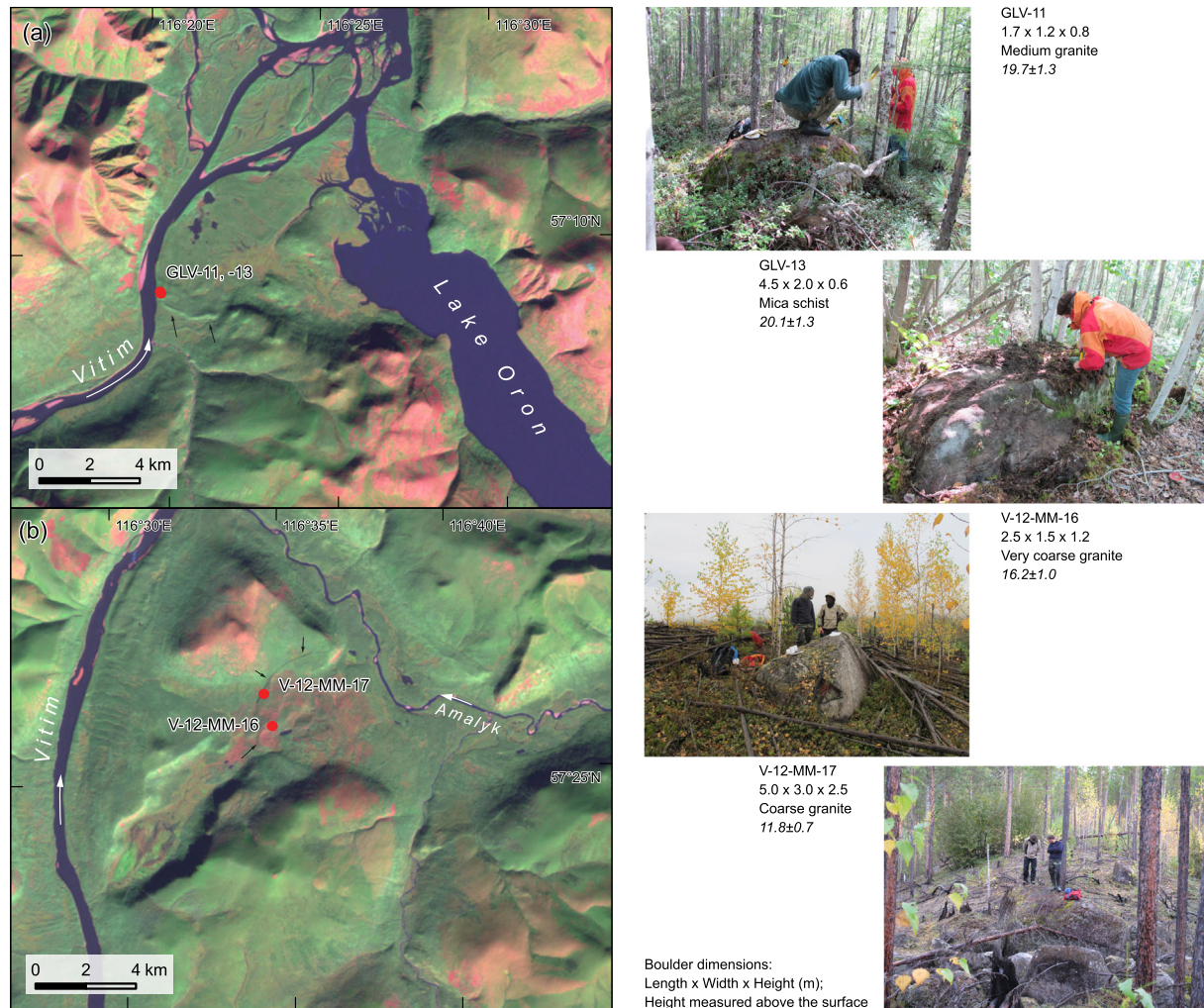


**Fig. 6.** Northwest slopes of the Kodar Mountains with sampling sites (red dots): Landsat image (LE71290212000275SGS00; channels 5, 3, 1) draped over SRTM data. (a) Oron delta moraine, (b) Baznyi moraine. The moraine ridges are marked by black arrows. Photographs to the right of the map panels show the sampled boulders. See Fig. 4 for the location of Fig. 6 map panels. (For interpretation of the references to colour in this figure legend, the reader is referred to the web version of this article.)

deposition behind a moraine in the Tamarak valley (Fig. 7a, d-f), 48 replicate measurements were carried out (2 mm aliquot size), and 32 of those passed the usual rejection criteria (Wintle and Murray, 2006). The distribution of De values was found to be relatively complex, implying the presence of partial bleaching in some of the aliquots. Using the Central Age Model results in an age of  $20.6 \pm 2.4$  ka, whereas the Minimum Age Model (MAM,  $\delta b = 0.20$ ) yields  $10.6 \pm 1.7$  ka (Table 2; cf. Galbraith et al., 1999). The true age of deposition is likely to fall between these two scenarios, but it would require a larger number of samples to better constrain the age estimates.

## 5. Discussion

### 5.1. Interpreting $^{10}\text{Be}$ concentrations in glacial landforms

The  $^{10}\text{Be}$  concentration measured in a boulder on a moraine crest reliably records the timing of glacial retreat assuming that the sampled surface: 1) does not contain cosmogenic nuclides inherited from an earlier ice-free interval; 2) has been continuously exposed sub-aerially since emergence from under ice and has not been shielded by sediment, snow or vegetation cover; 3) has not been repositioned or reoriented appreciably; and 4) has

experienced negligible erosion. The above factors fall into two categories: processes that lead to overestimation of the exposure age (1), and processes that make the modelled ages too young (2, 3, and 4). Such biases have been discussed in various studies that include distinctions as to which processes dominate a given study area depending on the mode of glaciation, and geomorphic and climatic setting (e.g., Gosse and Phillips, 2001; Fink et al., 2006; Balco, 2011; Heyman et al., 2011). It has been shown that bedrock surfaces are generally more prone to nuclide inheritance (Briner and Swanson, 1998; Stroeven et al., 2002), whereas incomplete exposure is more common for moraine boulders due to post-depositional disturbances (Heyman et al., 2011). For either case, surface erosion leads to loss of accumulated cosmogenic nuclides and hence a younger apparent exposure age, although weathering/erosion rate corrections (typically a few mm/ka) are generally minor for postglacially exposed surfaces (e.g. André, 2002). A correction for the cumulative effect of snow cover is difficult to gauge reliably over  $10^4$  y timescales (Schildgen et al., 2005), as is the influence of a forest canopy (Plug et al., 2007), though both will result in underestimation of the true exposure age (Gosse and Phillips, 2001). Here we apply no corrections to our measured  $^{10}\text{Be}$  concentrations to account for erosion or shielding and thus all modelled ages should be considered as minima.

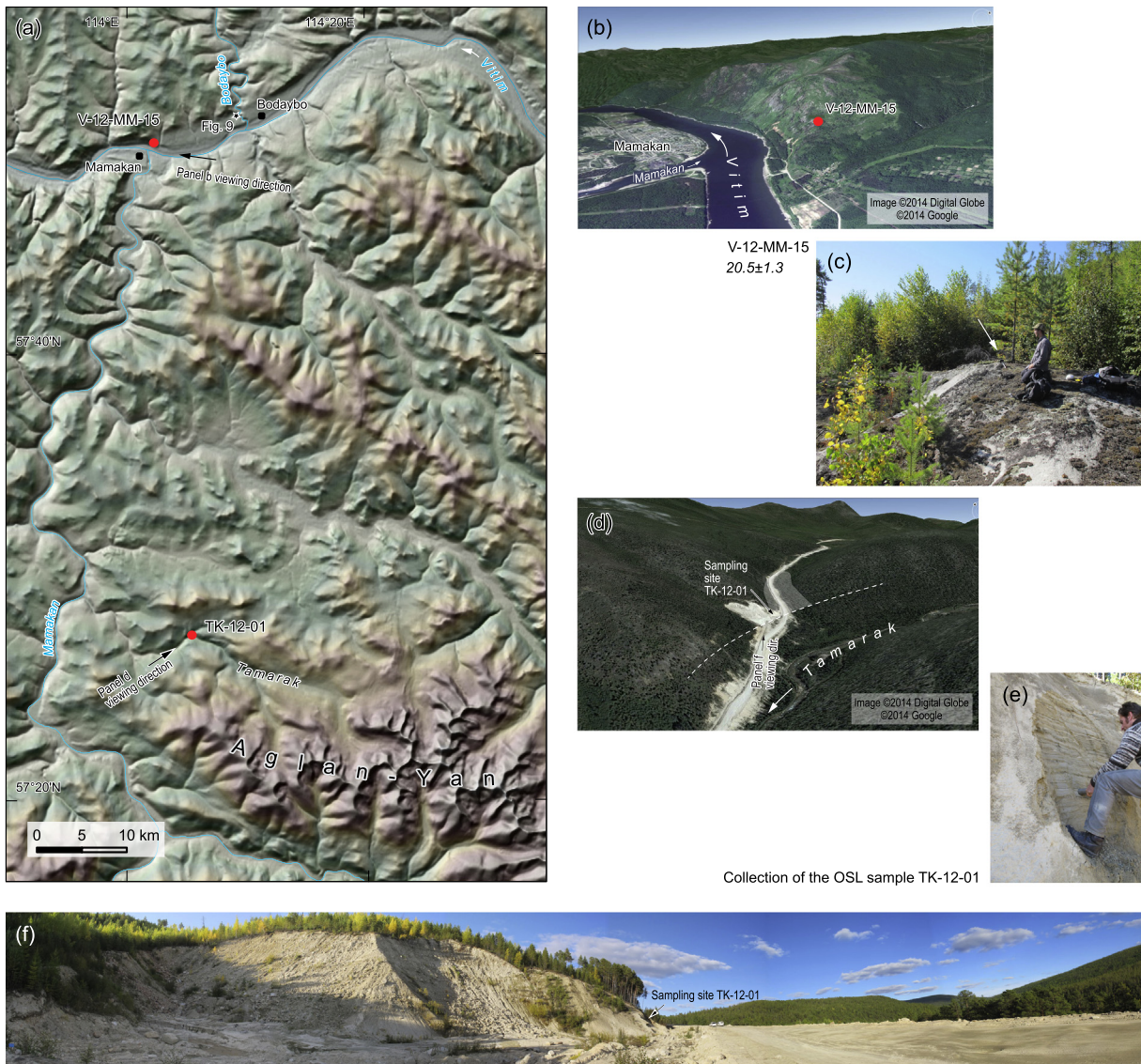


**Fig. 7.** (a) Bodaybo area, with sampling sites V-12-MM-15 and TK-12-01 (red dots), DEM-derived image (SRTM data). (b) Oblique Google Earth view on the confluence of the Vitim and Mamakan rivers and on the glacially modified slopes of the Vitim River valley. The site of sample V-12-MM-15 is drawn by a red dot and the viewing direction is indicated in panel a. (c) Photograph of the sampled glacially-scoured surface (ice flow direction into the image), the sampling site is indicated by a white arrow behind the person for scale. (d) Oblique Google Earth view of the Tamarak River valley with a site of OSL sample TK-12-01. The interpreted palaeo-configuration with a glacier lobe damming a minor lake is drawn by a dashed line (ice margin) and white tint (glacial lake). (e) Detail on the section of laminated sediments at the time of OSL sampling. (f) Panoramic view on the Tamarak site showing a road-side gravel pit with a ~20 m high section of upwards-coarsening diamiction. At the eastern end of the section, several metres of stratified sediment grade up from clayey-silts at base to silts with intercalated sandy beds, which we interpret as a minor proglacial lake sequence (see panel d for palaeo-configuration) from which OSL sample TK-12-01 was collected. (For interpretation of the references to colour in this figure legend, the reader is referred to the web version of this article.)

### 5.1.1. Glaciation in the high mountain ranges: Kodar and Udokan

The mapped geomorphology (Margold and Jansson, 2011), part of which includes the moraines sampled for exposure dating, indicates extensive mountain ice fields in the Kodar and Udokan mountains (Figs. 3 and 4). The two distinct generations of moraines on the southern slopes of the Udokan Mountains are an optimal target for investigation (see Fig. 3), but regrettably these were out of reach for logistical reasons. Instead, we focused on deciphering the chronology of glacial limits in the Chara Depression and on the northwest side of the Kodar Mountains. Whereas the glacial evidence northwest of the Kodar Mountains appears to be more complicated (we discuss this further in Section 5.1.2), the moraines in the Chara Depression represent terminal glacier positions. These massive moraines were formed by outlet glaciers of the Kodar and Udokan ice fields and some feature two distinct moraine ridges

(Fig. 5 a, b). In addition, a series of recessional moraines occur sporadically upstream of the terminal moraine complexes, for example, in the Sulban River valley (Fig. 4).

As noted above, the  $^{10}\text{Be}$  concentrations for multiple samples from a given single moraine spread over a range that cannot be explained by the far smaller analytical error for all the samples within the group. For example, the three samples from the Ikabja moraine (V-12-MM-7, -8, -9) give more than a twofold range in  $^{10}\text{Be}$  concentration yet each has a total analytical error <5% (Table 1). Therefore, the observed age spread must result from geological factors and some of the post-depositional processes mentioned above are strongly implicated. Unfortunately, the small number of samples measured for individual moraines does not allow for a more detailed quantitative interpretation of the ages, such as that suggested by Applegate et al. (2012). However, we can propose

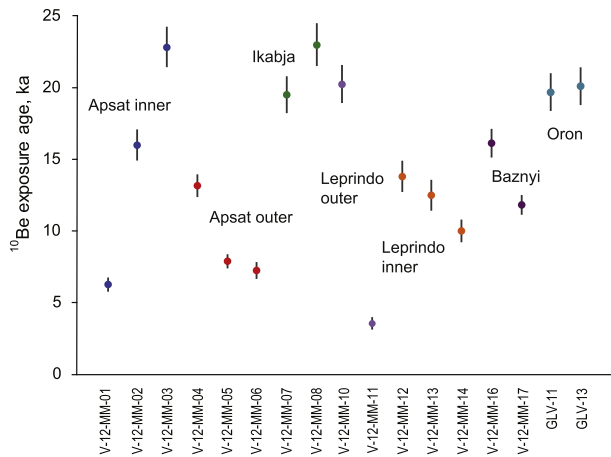


**Fig. 8.** Modelled  $^{10}\text{Be}$  exposure ages  $\pm 1 \sigma$  external uncertainty for the five moraine complexes. Note that sample V-12-MM-09 ( $42.7 \pm 3.8$  ka) is not shown.

qualitative interpretations that allow an age model to be selected, based on our judgement of the main active geomorphic processes. If the large spread in  $^{10}\text{Be}$  concentrations resulted from widespread and varied nuclide inheritance (despite this being rather uncommon; Heyman et al., 2011), then the youngest age for each deposit would be the more reliable as it would contain the lowest proportion of inheritance and therefore a minimum age model would be most appropriate. However, in that case, half of the sampled moraines would be of mid-Holocene age, which is highly implausible considering the available information on past climate and glacial chronologies from the wider region (Mackay, 2007; Shichi et al., 2009; Tarasov et al., 2009; Arzhannikov et al., 2012).

Alternatively, we infer that processes causing age underestimation have affected some of our samples. Several factors can be invoked. First, the study area lies within zones of continuous and discontinuous permafrost (Maurer, 2007); hence, permafrost dynamics have quite possibly contributed to post-depositional disturbance throughout the Late Glacial and Holocene. Moreover, the moraines might have been ice-cored (and possibly still are) and the buried ice may have experienced melting during the warmer-than-present climate of the early Holocene (Tarasov et al., 2009) resulting in alteration of the moraine morphology. Second, the existence of a temporary glacial lake has been documented in the Chara Depression (Enikeev, 2008, 2009; Margold and Jansson, 2011). The outer Apsat moraine crest has the lowest elevation of all moraines sampled in the Chara Depression and we observed glaciolacustrine sediments outcropping at the distal slope of the moraine ( $57.00155^\circ$  N,  $118.32108^\circ$  E). If a glacial lake submerged this moraine and others within the Chara Depression, wave erosion along shorelines could potentially modify and destabilize the moraine crests, leaving them prone to degradation even after drainage of the lake. Third, the degree of weathering among sampled boulders and blocks was highly variable. Whereas some surfaces appeared highly weathered, with weathering rinds and

certainly some loss of material, others were fresh, highly resistant to chiselling and without noticeable alteration of the rock surface. Nonetheless, no apparent relationship is discernible between the degree of weathering and the modelled exposure ages. Although variable erosion rates would result in scattered, depressed ages, any reasonable range of erosion rates acting continuously over the past 20–40 kyrs would not on its own explain the excessive spread in  $^{10}\text{Be}$  concentrations. Similarly, no relation is found between the height above ground surface of the sampled boulders and their modelled age, with the possible exception of sample V-12-MM-11, which was among the lowest free-standing heights and volumes and where the local surface morphology possibly indicates progressive surface degradation (see Fig. 5b).

We apply a maximum age model to our moraine boulder exposure ages to infer the timing of ice retreat. Considering the oldest age measured on each moraine: at Leprindo Lakes the outer moraine dates to  $\sim 20$  ka (i.e., matching the LGM), and the inner moraine crest dates to  $\sim 14$  ka (Fig. 5b); at the Apsat River moraine complex, all ages on the outer moraine crest must be rejected since they would make it younger than the inner crest and the inner moraine ridge is dated to  $\sim 23$  ka (i.e., again consistent with LGM age; Fig. 5a). Following the same logic, the Ikabja moraine (Fig. 5c) would date to  $\sim 48$  ka. However, here we argue that since sample V-12-MM-09 is more than two-times older than all others in our dataset, and the other two Ikabja samples fall within the LGM ( $\sim 23$  and  $\sim 20$  ka), this anomalously old sample is interpreted to reflect nuclide inheritance. Akin to the other two moraine complexes, the Ikabja moraine is thereby also attributed LGM age. Moving from the Chara Depression to the northwest slopes of the Kodar Mountains, the moraine in the Vitim River valley west of Lake Oron (Fig. 6a) matches with the LGM ( $\sim 20$  ka), while the Baznyi moraine (Fig. 6b) is of a Late Glacial age ( $\sim 16$  ka).

Our data illustrate the difficulty with conducting exposure age dating in active permafrost areas (cf. Zech et al., 2005; Stroeven et al., 2014). In opting for a maximum age model, we suggest our data support a glacial advance between 23 and 20 ka, commensurate with global LGM timing (Yokoyama et al., 2000; Clark et al., 2009), plus a possible Late Glacial readvance after  $\sim 16$  ka. Our mapping indicates that glaciers in the Kodar Mountains reached lengths of over 100 km (Fig. 3) at the LGM. This contrasts with the limited glacier extents reconstructed for the LGM in the regions farther east (Stauch et al., 2007; Stauch and Gualtieri, 2008; Stauch and Lehmkühl, 2010) and also with the south-eastern sector of the Barents-Kara Ice Sheet, which did not reach continental Siberia during OIS-2 (Svendsen et al., 2004).

### 5.1.2. Glaciation in the Bodaybo area

Whereas our data from the Kodar and Udokan mountains provide strong evidence for an LGM ice advance in the high massifs of Transbaikalia, the few data available from the Bodaybo area of the Vitim valley to the north-east (Fig. 7) allow only for some speculations on the broader regional glaciations. Margold and Jansson (2011) interpreted the Vitim valley as glacially modified for a substantial distance downstream of its passage through the high mountain region of the Northern-Muysk, Delyun-Uran, and Kodar

**Table 2**  
Summary OSL dating information (sample TK-12-01), with estimated water content (W) and measured concentration of dose-rate relevant elements (K, Th, U) used for calculation of the dose rate (D). Number of replicate measurements (n) and observed overdispersion (od.) as well as equivalent dose (De) for both CAM and MAM are listed together with the resulting ages.

Latitude	Longitude	Depth (cm)	Elevation (m)	Grain-size ( $\mu\text{m}$ )	W (%)	K (%)	Th (ppm)	U (ppm)	D ( $\text{Gy ka}^{-1}$ )	n	od.	De (Gy)	Age (ka)
57.4578	114.0901	300	630	63–100	$40 \pm 5$	$2.22 \pm 0.11$	$3.53 \pm 0.16$	$1.29 \pm 0.13$	$2.05 \pm 0.15$	32	0.49	$42.2 \pm 3.7$	$20.6 \pm 2.4$
											MAM	$21.6 \pm 3.0$	$10.6 \pm 1.7$

mountains (Figs. 2 and 3). Our field observations confirmed the glacial modification of the river valley and extended it downstream of Bodaybo where we observed bedrock glacial striations preserved beneath a thin sediment cover (57.846° N, 114.154° E; Fig. 9) near the junction of the Bodaybo and Vitim rivers.

The glacially-scoured hillslopes above the Vitim River near Mamakan show signs of local weathering and exfoliation, though our sampling site was carefully chosen from an intact glacially-scoured bedrock surface (Fig. 7c). It is likely that some surface weathering has occurred since glacial striations were not observed, and we cannot exclude the possibility that the sampled surface was for some time shielded by colluvium, which would lower its average  $^{10}\text{Be}$  production rate. In any case, our modelled exposure age of 21 ka is difficult to reconcile with the radiocarbon chronology indicating that the Vitim River valley at Bodaybo was ice-free at the time (see Section 2.1; Ineshin and Teten'kin, 2010). For ice to fill the Vitim valley downstream of Bodaybo a substantial glaciation is required, most likely in the form of an ice cap extending from the high mountains over the highlands east and south of Bodaybo (Fig. 10a). The existence of this ice cap at some prior stage is evident from the regional pattern of glacial modification, with areal scouring observed in the highlands north of the Vitim River (see Fig. 3; Margold and Jansson, 2011), and has been previously discussed in the literature (Obruchev, 1923, 1932; Logatchev, 1974; Zolotarev, 1974; Enikeev, 2009; Margold and Jansson, 2011).

Our OSL date from the Tamarak River valley (TK-12-01; Table 2, Fig. 7a, d-f) indicates that a glacier ~20 km in length descended from the Aglan-Yan Range at ~21 ka. Peaking at 1836 m asl, the Aglan-Yan Range is substantially lower than the higher massifs to the south, though it still bears evidence of mountain glaciation. Based on this single OSL age, we speculate that the Aglan-Yan Range and similar minor ranges to the north of the high mountain crux of Transbaikalia were heavily glaciated at the LGM (Fig. 10).

## 5.2. Comparison with previous glacial chronologies for Transbaikalia

Notwithstanding the debate concerning the multiplicity of earlier glaciations in Transbaikalia (see Section 2.1), our dating captures the OIS-2 glaciation only. According to the available regional climate records, derived from pollen and Lake Baikal diatoms, the coldest part of OIS-2 spans 26–20 ka (Müller et al., 2014) and thus coincides with the global LGM (Yokoyama et al., 2000; Clark et al., 2009). This period was not only colder but also drier than the preceding OIS-3 (Prokopenko et al., 2001; Mackay, 2007). Cold conditions remained until at least 14.5 ka (Shichi et al., 2009), followed by warmer and possibly wetter than present-day conditions at 14–13 ka (Shichi et al., 2009; Tarasov et al., 2009). Cooling then returned between 12.8 and 11.6 ka, during the Younger Dryas Chronozone (Mackay, 2007; Shichi et al., 2009; Tarasov et al., 2009).

Our data indicate that extensive glaciation existed during the coldest part of OIS-2 in the high mountains of Transbaikalia with a system of branching valley glaciers feeding from the Kodar Mountains into the Vitim valley and into the Chara Depression, which also received glaciers from the Udokan Range (Figs. 3 and 9). Whereas solid evidence exists for large LGM mountain ice fields on the highest massifs, the paucity of chronological constraints beyond the high mountains invites a more speculative view. The geomorphology is in clear support of an ice-cap glaciation to the northwest of the Kodar Mountains that filled the Vitim valley with ice for several hundreds of km, but the timing of this event is not firmly established. We note that the suggestions of a Middle or early Late Pleistocene glaciation from Logatchev (1974) and Zolotarev (1974) match the more recent glacial chronologies from the wider region that advocate diminishing ice extents leading up



Fig. 9. Glacial striations on a sediment covered bedrock surface (57.846° N, 114.154° E) near the junction of the Bodaybo and Vitim rivers. See Fig. 7a for the location.

to and including the LGM (Svendsen et al., 2004; Gillespie et al., 2008; Stauch and Gualtieri, 2008; Arzhannikov et al., 2012).

A crude estimate of LGM equilibrium line altitude (ELA) using a toe-to-headwall altitude ratio of 0.5 (Benn and Lehmkuhl, 2000) coupled with the elevation of the lowest preserved lateral moraines indicates a NW-SE altitudinal trend in ELA consistent with the precipitation gradient. ELA grew in height from ~975 m asl in the Aglan-Yan Range, to ~1500 m asl on the southern slopes of the Udokan Range (Fig. 10b). Indeed, for the region northwest of the Kodar Mountains an ELA at ~1000 m asl quite possibly provided sufficient accumulation area for an ice cap to develop. Nonetheless, given that we have just one date in favour of an LGM ice cap capable of supporting a Vitim valley glacier beyond Bodaybo, and that this date conflicts with the existing  $^{14}\text{C}$  dates from the area (albeit via potentially unreliable  $^{14}\text{C}$  measurements on bone; e.g., Stafford et al., 1987), we defer to future work on the question of the regional ice-cap style glaciation.

## 5.3. A Late Glacial readvance?

A final question that remains difficult to resolve with our data concerns the Late Glacial readvances and their extent. Notwithstanding Mackay's (2007, p. 198) view that "the transition from the end of the last glacial into the Holocene (Termination 1) was rapid in Lake Baikal (only c. 4 ka)", climate reconstructions elsewhere indicate that conditions remained cold until ~14.5 ka, then cooled again after warming briefly at 14.5–13 ka, coincident with the

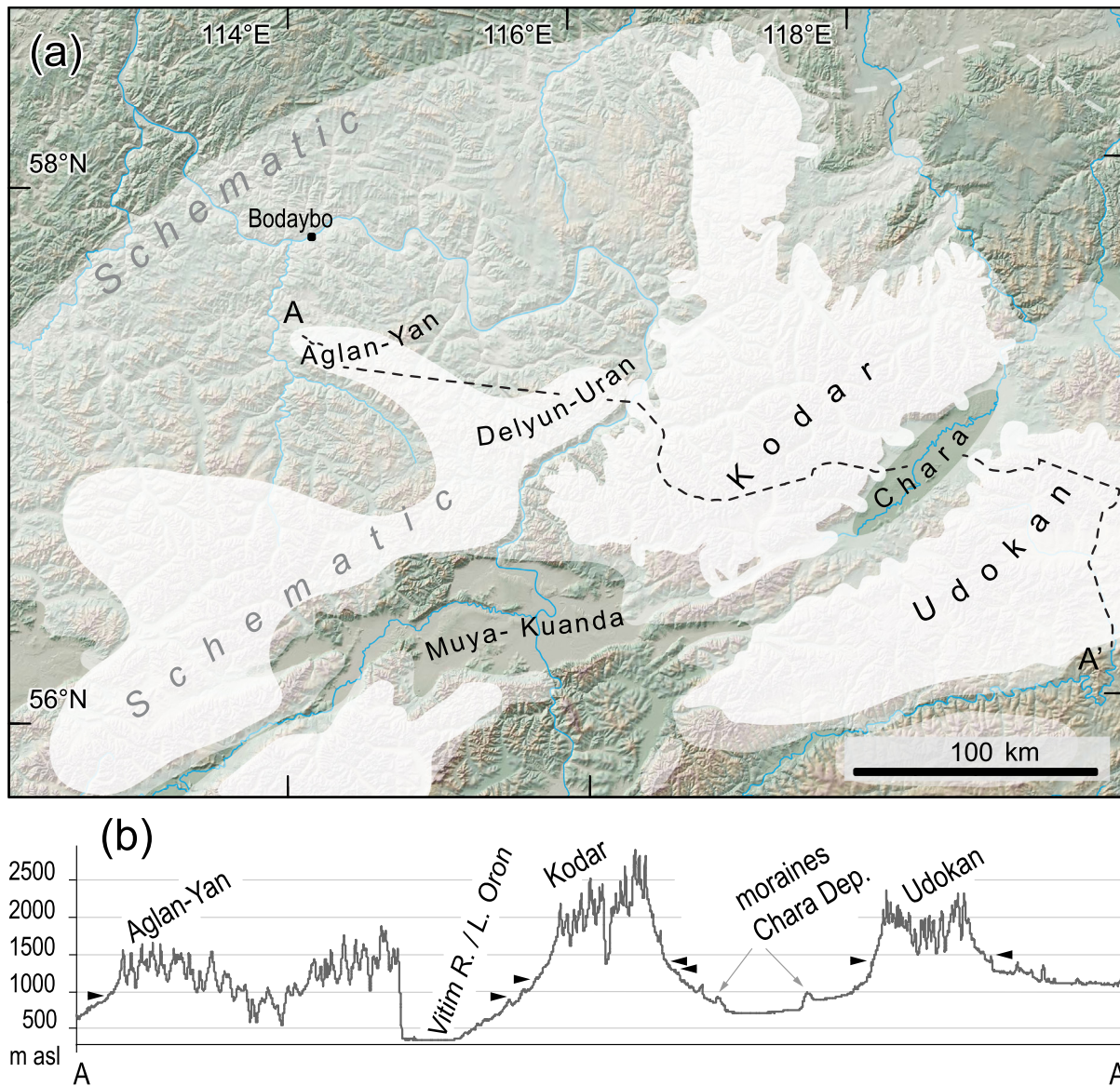


**Fig. 10.** (a) Schematic reconstruction of LGM ice extent (white) in central Transbaikalia; note that except for the southeast flanks of the Kodar Mountains the ice extent shown is speculative. Large valley glaciers were fed from a hypothesised ice field that spanned the Kodar and lower mountains to the north with a similar ice field mapped also in the Udokan Mountains. Evidence of a more extensive, ice-cap type glaciation (white tint) occurs northwest of the highest massifs, but the timing of this glaciation remains unconfirmed (see main text). Dashed black line indicates vertical transect A–A' pictured in panel b. (b) Reconstructed approximate elevation of the equilibrium line altitude (ELA) across the NW-SE transect through the study area (marked by black arrows). Note the successively higher ELAs corresponding to a precipitation gradient between the wetter NW portion and the drier, more continental SE portion of the study area.

Bølling-Allerød interstadial (Shichi et al., 2009; Tarasov et al., 2009). Unfortunately, the large spread in our moraine boulder exposure ages makes it difficult to provide a reliable conclusion on the presence of a Late Glacial ice re-advance in the study area. With this caveat stated, following a maximum age model for our moraines (excepting the inheritance in V-12-MM-09) yields an LGM age for the inner Apsat, outer Leprindo, Ikabja, and Oron moraines, whereas the Baznyi and inner Leprindo moraines are attributed to a Late Glacial advance. Interestingly, the latter two 'Late Glacial' moraines attest to an ice extent similar to that of the 'LGM' moraines. We note that a similar pattern has recently been reported from the Khangai Mountains of Mongolia (Fig. 1), where an ice re-advance at 17–16 ka reached within 1–2 km of the local LGM limits (Rother et al., 2014). In addition, evidence of minor still-stands or

re-advances of glaciers higher in the mountains exists in the form of recessional moraines in some mountain valleys (Fig. 4). Such sites remained out of reach during our 2011 and 2012 field expeditions, leaving much further work yet to be done.

## 6. Conclusions

We applied cosmogenic  $^{10}\text{Be}$  exposure dating to glacial landforms with the aim of investigating the glacial history of central Transbaikalia. A set of eighteen  $^{10}\text{Be}$  exposure ages were determined from five moraine complexes emanating from the Kodar and Udokan mountains. Our results indicate a major glaciation involving extensive mountain ice fields in the highest massifs during OIS-2, coincident with the global LGM. The relatively large

spread among the exposure ages is most likely due to incomplete exposure caused by post-depositional disturbance of the moraines. Whereas two of the investigated moraines date to the Late Glacial and minor recessional moraines do occur higher in the mountains, the issue of incomplete boulder exposure compromises our ability to specify the precise timing of a Late Glacial re-advance in the region.

Strong evidence exists for an even more extensive ice-cap type glaciation northwest of the Kodar Mountains. We argue, on the basis of OSL-dated glacial sediments, that even the lower mountains to the north of the highest massifs were heavily glaciated at the LGM. Although a single  $^{10}\text{Be}$  exposure age in support of the ice cap also indicates an LGM age, this conflicts with existing radiocarbon ages recording ice-free conditions at the Vitim River near Bodaybo at the time (Ineshin and Teten'kin, 2010). A suggested pre-OIS-2 timing for this extensive regional glaciation would be consistent with the trend of successively smaller glaciations since OIS-6, previously reconstructed in northern and northeastern Eurasia (Svendsen et al., 2004; Stauch and Gualtieri, 2008; Arzhannikov et al., 2012). Suffice to say that compelling evidence exists for large ice fields in the mountains of Transbaikalia at the LGM, but the timing of an even more extensive, regional ice-cap glaciation has yet to be established.

### Acknowledgements

We thank Anton Brichevskiy for his help during the 2012 field season and our thanks extend to the staff of the Vitim Nature Reserve. We further thank Steven A. Binnie for arranging the measurement of samples GLV-11 and GLV-13 at the University of Cologne AMS laboratory. Finally, we thank Julie Brigham-Grette and an anonymous reviewer for their constructive comments on an earlier version of the manuscript.

This work was supported by funding from the Swedish Society for Anthropology and Geography, the Bolin Centre for Climate Research, the Royal Swedish Academy of Sciences (FOA12Althin-034), Stockholm University, and Stiftelse YMER-80 to Martin Margold; and by funding from the Australian Institute of Nuclear Science and Engineering (ALNGRA12021P) and the Australian Research Council (DP130104023) to John Jansen.

### Appendix A. Supplementary data

Supplementary data related to this article can be found at <http://dx.doi.org/10.1016/j.quascirev.2015.11.018>.

### References

- André, M.-F., 2002. Rates of postglacial rock weathering on glacially scoured outcrops (Abisko-Riksgränsen area, 68°N). *Geogr. Ann.* 84 A, 3–4.
- Applegate, P.J., Urban, N.M., Keller, K., Lowell, T.V., Laabs, B.J.C., Kelly, M.A., Alley, R.B., 2012. Improved moraine age interpretations through explicit matching of geomorphic process models to cosmogenic nuclide measurements from single landforms. *Quat. Res.* 77, 293–304.
- Arzhannikov, S.G., Braucher, R., Jolivet, M., Arzhannikova, A.V., Vassallo, R., Chauvet, A., Bourlès, D., Chauvet, F., 2012. History of late Pleistocene glaciations in the central Sayan-Tuva Upland (Southern Siberia). *Quat. Sci. Rev.* 49, 16–32.
- Astakhov, V.I., 2013. Pleistocene glaciations of Northern Russia—a modern view. *Boreas* 42, 1–24.
- Balco, G., 2011. Contributions and unrealized potential contributions of cosmogenic nuclide exposure dating to glacier chronology, 1990–2010. *Quat. Sci. Rev.* 30, 3–27.
- Balco, G., Stone, J.O., Lifton, N.A., Dunai, T.J., 2008. A complete and easily accessible means of calculating surface exposure ages or erosion rates from  $^{10}\text{Be}$  and  $^{26}\text{Al}$  measurements. *Quat. Geochronol.* 3, 174–195.
- Barr, I.D., Clark, C.D., 2011. Glaciers and climate in Pacific far NE Russia during the last glacial maximum. *J. Quat. Sci.* 26, 227–237.
- Barr, I.D., Clark, C.D., 2012. An updated moraine map of Far NE Russia. *J. Maps* 8, 431–436.
- Bazarov, D.B., 1986. The Cenozoic of Cisbaikalia and Western Transbaikalia. *Nauka, Novosibirsk* (in Russian).
- Bazarov, D.B., Rezanov, I.N., Budaev, R.C., Imethenov, A.B., et al., 1981. The Geomorphology of Northern Cisbaikalia and the Stanovoe Range. *Nauka, Moscow* (in Russian).
- Benn, D.I., Lehmkühl, F., 2000. Mass balance and equilibrium-line altitudes of glaciers in high-mountain environments. *Quat. Int.* 65–66, 15–29.
- Bigg, G.R., Clark, C.D., Hughes, A.L.C., 2008. A last glacial ice sheet on the Pacific Russian coast and catastrophic change arising from coupled ice–volcanic interaction. *Earth Planet. Sci. Lett.* 265, 559–570.
- Brigham-Grette, J., 2001. New perspectives on Beringian quaternary paleogeography, stratigraphy, and glacial history. *Quat. Sci. Rev.* 20, 15–24.
- Briner, J.P., Swanson, T.W., 1998. Using inherited cosmogenic  $^{36}\text{Cl}$  to constrain glacial erosion rates of the Cordilleran ice sheet. *Geology* 26, 3–6.
- Child, D., Elliott, G., Mifsud, C., Smith, A.M., Fink, D., 2000. Sample processing for earth science studies at ANTARES. *Nucl. Instrum. Methods Phys. Res. Sect. B Beam Interact. Mater. Atoms* 172, 856–860.
- Chmeleff, J., von Blanckenburg, F., Kossert, K., Jakob, D., 2010. Determination of the  $^{10}\text{Be}$  half-life by multicollector ICP-MS and liquid scintillation counting. *Nucl. Instrum. Methods Phys. Res. Sect. B* 268, 192–199.
- Clark, P.U., Dyke, A.S., Shakun, J.D., Carlson, A.E., Clark, J., Wohlfarth, B., Mitrovica, J.X., Hostetler, S.W., McCabe, A.M., 2009. The last glacial maximum. *Science* 325, 710–714.
- Dewald, A., Heinze, S., Jolie, J., et al., 2013. CologneAMS, a dedicated center for accelerator mass spectrometry in Germany. *Nucl. Instrum. Methods Phys. Res. B* 294, 18–23.
- Enikeev, F.I., 2008. The Late Cenozoic of northern Transbaikalia and paleoclimates of southern East Siberia. *Russ. Geol. Geophys.* 49, 602–610.
- Enikeev, F.I., 2009. Pleistocene glaciations in the East Transbaikalia and the Southeast of Middle Siberia. *Geomorfologiya* 40, 33–49 (In Russian).
- Fink, D., McKelvey, B., Hambrey, M.J., Fabel, D., Brown, R., 2006. Pleistocene deglaciation chronology of the Amery Oasis and Radok Lake, Northern Prince Charles mountains, Antarctica. *Earth Planet. Sci. Lett.* 243, 229–243.
- Fink, D., Smith, A., 2007. An inter-comparison of  $^{10}\text{Be}$  and  $^{26}\text{Al}$  AMS reference standards and the  $^{10}\text{Be}$  half-life. *Nucl. Instrum. Methods Phys. Res. Sect. B Beam Interact. Mater. Atoms* 259, 600–609.
- Galbraith, R.F., Roberts, R.G., Laslett, G.M., Yoshida, H., Olley, J.M., 1999. Optical dating of single and multiple grains of quartz from Jinnium rock shelter, northern Australia: Part I, experimental design and statistical models. *Archaeometry* 41, 339–364.
- Geniatulin, R.F., 2000. The Encyclopedia of Transbaikalia: Chita Region. *Nauka, Novosibirsk* (In Russian).
- Gillespie, A.R., Burke, R.M., Komatsu, G., Bayasgalan, A., 2008. Late pleistocene glaciers in Darhad Basin, Northern Mongolia. *Quat. Res.* 69, 169–187.
- Gosse, J.C., Phillips, F.M., 2001. Terrestrial in situ cosmogenic nuclides: theory and application. *Quat. Sci. Rev.* 20, 1475–1560.
- Heyman, J., 2014. Paleoglaciation of the Tibetan Plateau and surrounding mountains based on exposure ages and ELA depression estimates. *Quat. Sci. Rev.* 91, 30–41.
- Heyman, J., Stroeven, A.P., Harbor, J.M., Caffee, M.W., 2011. Too young or too old: evaluating cosmogenic exposure dating based on an analysis of compiled boulder exposure ages. *Earth Planet. Sci. Lett.* 302, 71–80.
- Ineshin, E.M., Teten'kin, A.V., 2010. Human and Environment in the North of Baikalian Siberia in Late Pleistocene. *Archaeological site Bol'shoi Iakor' I, Nauka, Novosibirsk* (In Russian).
- Kohl, C., Nishiizumi, K., 1992. Chemical isolation of quartz for measurement of in situ-produced cosmogenic nuclides. *Geochimica Cosmochimica Acta* 6, 3583–3587.
- Kolomiets, V.L., 2008. Paleogeography and quaternary terrace sediments and complexes, intermontane basins of Prebaikalia (Southeastern Siberia, Russia). *Quat. Int.* 179, 58–63.
- Komatsu, G., Arzhannikov, S.G., Arzhannikova, A.V., Ershov, K., 2007a. Geomorphology of subglacial volcanoes in the Azas Plateau, the Tuva Republic, Russia. *Geomorphology* 88, 312–328.
- Komatsu, G., Arzhannikov, S.G., Arzhannikova, A.V., Ori, G.G., 2007b. Origin of glacial–fluvial landforms in the Azas Plateau volcanic field, the Tuva Republic, Russia: role of ice–magma interaction. *Geomorphology* 88, 352–366.
- Korschinek, G., Bergmaier, A., Faestermann, T., Gerstmann, U.C., Knie, K., Rugela, G., Wallner, A., Dillmann, I., Dollinger, G., Lierse von Gostomsk, Ch, Kossert, K., Maitia, M., Poutivtseva, M., Remmer, A., 2010. A new value for the half-life of  $^{10}\text{Be}$  by heavy ion elastic recoil detection and liquid scintillation counting. *Nucl. Instrum. Methods Phys. Res. Sect. B* 268, 187–191.
- Kropotkin, P.A., 1876. Studies on the ice age. *Pap. Russ. Geogr. Soc.* 7, 1–837 (In Russian).
- Krivonogov, S.K., Takahara, H., 2003. In: Kamata, N. (Ed.), Late Pleistocene and Holocene Environmental Changes Recorded in the Terrestrial Sediments and Landforms of Eastern Siberia and North Mongolia, Proceedings of International Symposium of the Kanazawa University 21st-Century COE Program, vol. 1, pp. 30–36.
- Kulchitskiy, A.A., Skovitina, T.M., Ufimtsev, G.F., 1995. The ability to quickly flood the bottom of the Muya basin by a collapsing ravine in the Parama Canyon of the Vitim. *Environ. Aspects Theor. Appl. Geomorphol. Proc. Int. Conf. "III Shchukin Read."* 136–137 (In Russian).
- Kulchitskiy, A.A., Panychev, V.A., Orlova, L.A., 1990. Late Pleistocene deposits of the Muya-Kuanda depression and their rate of accumulation. In: 7th Union Conference on Quaternary Research “Quaternary Period: Research Methods, Stratigraphy and Ecology”, Tallin, pp. 112–113 (In Russian).

- Lal, D., 1991. Cosmic ray labeling of erosion surfaces: in situ nuclide production rates and erosion models. *Earth Planet. Sci. Lett.* 104, 424–439.
- Lehmkuhl, F., Klinge, M., Stauch, G., 2004. The extent of Late Pleistocene glaciations in the Altai and Khangai mountains. In: Ehlers, J., Gibbard, P.L. (Eds.), *Developments in Quaternary Sciences*. Elsevier, pp. 243–254.
- Lehmkuhl, F., Klinge, M., Stauch, G., 2011. Chapter 69-The extent and timing of late pleistocene glaciations in the Altai and neighbouring mountain systems. In: Jürgen Ehlers, P.L.G., Philip, D.H. (Eds.), *Developments in Quaternary Sciences*. Elsevier, pp. 967–979.
- Lehmkuhl, F., Zander, A., Frechen, M., 2007. Luminescence chronology of fluvial and aeolian deposits in the Russian Altai (Southern Siberia). *Quat. Geochronol.* 2, 195–201.
- Logatchev, N.A., 1974. Sayan-baikal Upland. In: Florensov, N.A. (Ed.), *The Highlands of Cisbaikalia and Transbaikalia*. Nauka, Moscow (In Russian).
- Mackay, A.W., 2007. The paleoclimatology of Lake Baikal: a diatom synthesis and prospectus. *Earth-Science Rev.* 82, 181–215.
- Mangerud, J., Jakobsson, M., Alexanderson, H., Astakhov, V., Clarke, G.K.C., Henriksen, M., Hjort, C., Krinner, G., Lunkka, J.P., Möller, P., Murray, A., Nikolskaya, O., Saarnisto, M., Svendsen, J.L., 2004. Ice-dammed lakes and rerouting of the drainage of Northern Eurasia during the last Glaciation. *Quat. Sci. Rev.* 23, 1313–1332.
- Margold, M., Jansson, K.N., 2011. Glacial geomorphology and glacial lakes of central Transbaikalia, Siberia, Russia. *J. Maps* 7, 18–30.
- Margold, M., Jansson, K.N., Stroeven, A.P., Jansen, J.D., 2011. Glacial Lake Vitim, a 3000-km<sup>2</sup> outburst flood from Siberia to the Arctic Ocean. *Quat. Res.* 76, 393–396.
- Maurer, J., 2007. Atlas of the Cryosphere. National Snow and Ice Data Center. Digital media, Boulder, Colorado USA.
- Mifsud, C., Fujioka, T., Fink, D., 2013. Extraction and purification of quartz in rock using hot phosphoric acid for in situ cosmogenic exposure dating. *Nucl. Instrum. Methods Phys. Res. Sect. B Beam Interact. Mater. Atoms* 294 (C), 203–207.
- Müller, S., Tarasov, P.E., Hoelzmann, P., Bezrukova, E.V., Kossler, A., Krivonogov, S.K., 2014. Stable vegetation and environmental conditions during the last glacial maximum: new results from Lake Kotokel (Lake Baikal region, Southern Siberia, Russia). *Quat. Int.* 348, 14–24.
- Murray, A.S., Wintle, A.G., 2000. Luminescence dating of quartz using an improved single-aliquot regenerative-dose protocol. *Radiat. Meas.* 32, 57–73.
- Nishizumi, K., Imamura, M., Caffee, M.W., Southon, J.R., Finkel, R.C., McAninch, J., 2007. Absolute calibration of <sup>10</sup>Be AMS standards. *Nucl. Instrum. Methods Phys. Res. B* 259, 403–413.
- Obruchev, V.A., 1923. Olekma-vitim Gold-bearing Region. In: *The Geological Review of Gold-bearing Regions of Siberia*. Lenzoloto, Moscow (In Russian).
- Obruchev, V.A., 1929. On the glaciation of the central Vitim mountain region. *Geogr. Bull.* 6 (4–6), 42–45 (In Russian).
- Obruchev, V.A., 1932. A Geological Sketch of Cisbaikalia and the Lena Area. *Essays on the Geology of Siberia*. The Academy of Sciences of the USSR, Leningrad.
- Osadchij, S.S., 1979. Limno-glacial conditions and the issues of correlation of the Pleistocene formations in the depressions of the Stanovoe Highlands, the history of lakes in the USSR in the late Cenozoic. In: *Materials for the 5th All-union Symposium, Part 2 (Central Siberia, Cisbaikalia, Transbaikalia, Yakutia, the Far East)*. Irkutsk, pp. 122–126 (In Russian).
- Osadchij, S.S., 1982. On the Problem of the Relation of Glacial and Fluvial Epochs on the Territory of Northern Transbaikalia, Late Cenozoic History of Lakes in the USSR. *Nauka, Novosibirsk* (In Russian).
- Osipov, E. Yu., Osipova, O.P., 2014. Mountain glaciers of southeast Siberia: current state and changes since the Little ice age. *Ann. Glaciol.* 55, 167–176.
- Plug, L.J., Gosse, J.C., McIntosh, J.J., Bigley, R., 2007. Attenuation of cosmic ray flux in temperate forest. *J. Geophys. Res.* 112, F02022.
- Preobrazhenskiy, V.S., 1960. Kodarskiy lednikovyy rayon (Zabaykal'ya) ([The Kodarsky glacier region (Transbaikal)]). *Nauka. Akademiia Nauk SSSR, Moscow* (Russian with English summary).
- Prokopenko, A.A., Karabanov, E.B., Williams, D.F., Kuzmin, M.I., Khursevich, G.K., Gvozdkov, A.A., 2001. The detailed record of climatic events during the past 75,000 yrs BP from the Lake Baikal drill core BDP-93-2. *Quat. Int.* 80–81, 59–68.
- Reimer, P.J., Bard, E., Bayliss, A., Beck, J.W., Blackwell, P.G., Bronk Ramsey, C., Buck, C.E., Cheng, H., Edwards, R.L., Friedrich, M., Grootes, P.M., Guilderson, T.P., Haffidason, H., Hajdas, I., Hatté, C., Heaton, T.J., Hoffmann, D.L., Hogg, A.G., Hughen, K.A., Kaiser, K.F., Kromer, B., Manning, S.W., Niu, M., Reimer, R.W., Richards, D.A., Scott, E.M., Southon, J.R., Staff, R.A., Turney, C.S.M., van der Plicht, J., 2013. IntCal13 and Marine13 radiocarbon age calibration curves 0–50,000 Years cal BP. *Radiocarbon* 55, 1869–1887.
- Rother, H., Lehmkuhl, F., Fink, D., Nottbaum, V., 2014. Surface exposure dating reveals MIS-3 glacial maximum in the Khangai mountains of Mongolia. *Quat. Res.* 82, 297–308.
- Shieldgen, T.F., Phillips, W.M., Purves, R.S., 2005. Simulation of snow shielding corrections for cosmogenic nuclide surface exposure studies. *Geomorphology* 64, 67–85.
- Shahgedanova, M., Mikhailov, N., Larin, S., Bredikhin, A., 2002. The mountains of Southern Siberia. In: Shahgedanova, M. (Ed.), *The Physical Geography of Northern Eurasia*. Oxford University Press, Oxford, pp. 314–349.
- Shahgedanova, M., Popovnin, V., Aleynikov, A., Stokes, C.R., 2011. Geodetic mass balance of Azarova glacier, Kodar mountains, Eastern Siberia, and its links to observed and projected climatic change. *Ann. Glaciol.* 52, 129–137.
- Shichi, K., Takahara, H., Krivonogov, S.K., Bezrukova, E.V., Kashiwaya, K., Takehara, A., Nakamura, T., 2009. Late Pleistocene and Holocene vegetation and climate records from Lake Kotokel, central Baikal region. *Quat. Int.* 205, 98–110.
- Stafford, T., Jull, A.T., Brendel, K., Duhamel, R.C., Donahue, D., 1987. Study of bone radiocarbon dating accuracy at the university of Arizona NSF accelerator facility for radioisotope analysis. *Radiocarbon* 29, 24–44.
- Stauch, G., Gualtieri, L., 2008. Late quaternary glaciations in northeastern Russia. *J. Quat. Sci.* 23, 545–558.
- Stauch, G., Lehmkuhl, F., 2010. Quaternary glaciations in the Verkhoyansk mountains, Northeast Siberia. *Quat. Res.* 74, 145–155.
- Stauch, G., Lehmkuhl, F., Frechen, M., 2007. Luminescence chronology from the Verkhoyansk mountains (North-Eastern Siberia). *Quat. Geochronol.* 2, 255–259.
- Stokes, C.R., Shahgedanova, M., Evans, I.S., Popovnin, V.V., 2013. Accelerated loss of alpine glaciers in the Kodar Mountains, South-eastern Siberia. *Glob. Planet. Change* 101, 82–96.
- Stone, J.O., 2000. Air pressure and cosmogenic isotope production. *J. Geophys. Res.* 105, 23753–23759.
- Stroeven, A.P., Fabel, D., Harbor, J., Hättstrand, C., Kleman, J., 2002. Quantifying the erosional impact of the Fennoscandian ice sheet in the Torneträsk-Narvik corridor, Northern Sweden, based on cosmogenic radionuclide data. *Geogr. Ann.* 84A, 275–287.
- Stroeven, A.P., Fabel, D., Margold, M., Clague, J.J., Xu, S., 2014. Investigating absolute chronologies of glacial advances in the NW sector of the Cordilleran ice sheet with terrestrial in situ cosmogenic nuclides. *Quat. Sci. Rev.* 92, 429–443.
- Stuiver, M., Reimer, P.J., 1993. Extended 14C database and revised CALIB radiocarbon calibration program. *Radiocarbon* 35, 215–230.
- Svendsen, J.L., Alexanderson, H., Astakhov, V.I., Demidov, I., Dowdeswell, J.A., Funder, S., Gataullin, V., Henriksen, M., Hjort, C., Houmark-Nielsen, M., Hubberten, H.W., Ingolfsson, O., Jakobsson, M., Kjaer, K.H., Larsen, E., Lokrantz, H., Lunkka, J.P., Lysa, A., Mangerud, J., Matiouchkov, A., Murray, A., Møller, P., Niessen, F., Nikolskaya, O., Polyak, L., Saarnisto, M., Sievert, C., Siegert, M.J., Spielhagen, R.F., Stein, R., 2004. Late quaternary ice sheet history of Northern Eurasia. *Quat. Sci. Rev.* 23, 1229–1271.
- Tarasov, P.E., Bezrukova, E.V., Krivonogov, S.K., 2009. Late Glacial and Holocene changes in vegetation cover and climate in southern Siberia derived from a 15 kyr long pollen record from Lake Kotokel. *Clim. Past.* 5, 285–295.
- Ufimtsev, G.F., Skovitina, T.M., Kulchitskiy, A.A., 1998. Rockfall-dammed lakes in the Baikal region: evidence from the past and prospects for the future. *Nat. Hazards* 18, 167–183.
- von Blanckenburg, F., Belshaw, N., O'Nions, R., 1996. Separation of Be-9 and cosmogenic Be-10 from environmental materials and SIMS isotope dilution analysis. *Chem. Geol.* 129, 93–99.
- von Blanckenburg, F., Hewawasam, T., Kubik, P.W., 2004. Cosmogenic nuclide evidence for low weathering and denudation in the wet, tropical highlands of Sri Lanka. *J. Geophys. Res.* Earth Surf. 109 (F3), F03008.
- Wintle, A.G., Murray, A.S., 2006. A review of quartz optically stimulated luminescence characteristics and their relevance in single-aliquot regeneration dating protocols. *Radiat. Meas.* 41, 369–391.
- Yokoyama, Y., Lambeck, K., De Deckker, P., Johnston, P., Fifield, L.K., 2000. Timing of the last Glacial maximum from observed sea-level minima. *Nature* 406, 713–716.
- Zech, R., Glaser, B., Sosin, P., Kubik, P.W., Zech, W., 2005. Evidence for long-lasting landform surface instability on hummocky moraines in the Pamir mountains (Tajikistan) from <sup>10</sup>Be surface exposure dating. *Earth Planet. Sci. Lett.* 237, 453–461.
- Zhao, J., Yin, X., Harbor, J.M., Lai, Z., Liu, S., Li, Z., 2013. Quaternary glacial chronology of the Kanas river valley, Altai mountains, China. *Quat. Int.* 311, 44–53.
- Zolotarev, A.G., 1974. The Baikal-Patom Upland. In: Florensov, N.A. (Ed.), *The Highlands of Cisbaikalia and Transbaikalia*. Nauka, Moscow (In Russian).